Computational and Theoretical Chemistry 998 (2012) 183–192

Contents lists available at SciVerse ScienceDirect

Computational and Theoretical Chemistry

journal homepage: www.elsevier.com/locate/comptc

Dimers and trimers of formamidine and its mono-halogenated analogues HN=CHNHX, (X = H, Cl, Br, or I): A comparative study of resonance-assisted hydrogen and halogen bonds

Ruben D. Parra *

Department of Chemistry, DePaul University 1110 W. Belden Ave., Chicago, IL 60614, United States

ARTICLE INFO

Article history:
Received 17 May 2012
Received in revised form 29 June 2012
Accepted 18 July 2012
Available online 7 August 2012

Keywords:
Halogen bonding
Hydrogen bonding
Formamidine
Ab initio
Density functional theory

ABSTRACT

The MP2 ab initio method, and the M052X and the B3LYP density functional theory methods were used to investigate the geometries and energetics of dimers and trimers of formamidine and its mono-halogenated analogues. The primary purpose of this study is to examine the strength of the resonance-assisted N—X···N interactions for X = H (hydrogen bond), relative to that for X = Cl, Br, or I (halogen bond). It is found that, for the dimers and trimers studied here, the hydrogen bond interaction is stronger than the halogen bond interactions when the halogen is either Cl or Br. For dimers, the N—H···N interaction is actually of comparable strength to that of the N—I···N interaction. For example, at the MP2 level the N—H···N interaction energy is −7.47 kcal/mol, and the corresponding N—I···N interaction energy is found to be −7.13 kcal/mol. Trimerization produces a small decrease in the hydrogen bond strength, with a hydrogen bond energy of −6.90 kcal/mol at the MP2 level. The opposite is true for the halogen bonds which actually get stronger upon trimer formation, not all to the same extent though. At the MP2 level, for instance, the magnitudes of the interaction energies increase by factors of 1.28 and 1.98 for N—Cl···N and N—Br···N respectively. A much more substantial increase factor of 3.36 is found in the N—I···N interaction energy upon trimer formation. The strengthening of the N—I···N interaction is so dramatic that the iodine is found midway between the two nitrogen atoms, and the interaction in the trimer is better described as a symmetric N···I···N interaction.

1. Introduction

The pivotal role that non-covalent interactions play in chemistry, biochemistry, and materials science is well recognized by the scientific community at large [1–4]. Without a doubt, the most investigated of these interactions is the highly directional hydrogen bond interaction. In the almost 100 years since its inception in the literature [5], the term hydrogen bond has been the subject of a great many books, see for example [6–10] for some current contributions, and a myriad of research publications that can be seen, for example, in a number of recent review articles [11–19]. Despite the long history and the many publications using the term hydrogen bond, it should be noted that the lack of a universally accepted understanding of what constitutes a hydrogen bond has been the source of some controversies. See for example the reviews on blue-shifting in hydrogen bonds [15,16], or the issue of weak and non-conventional hydrogen bonds [8,17,18]. To provide a common conceptual framework to discuss the hydrogen bond, an IUPAC Technical Report was released very recently where the following definition is recommended [20,21]: *The hydrogen bond is an attractive interaction between a hydrogen atom from a molecule or a molecular fragment X—H in which X is more electronegative than H, and an atom or a group of atoms in the same or a different molecule, in which there is evidence of bond formation.* The report was released by a Task Group charged with categorizing hydrogen bonding and other intermolecular interactions. The Task Group considered what is currently known, experimentally and theoretically, about the hydrogen bond as a basis for the recommended definition. The Task Group also acknowledges that the criteria and characteristics used to define a hydrogen bond are likely to evolve with the advent of new theoretical and experimental techniques. In fact, in a recent review, Grabowski discusses the issue of covalency in hydrogen bonding using geometry, energetic, natural bond orbital, and atoms in molecules or topological analysis criteria [19]. Sánchez-Sanz et al. have recently proposed the use of fragment based method to estimate electron density shifts to investigate non-bonding intramolecular interactions including hydrogen bonds, N···Br, halogen–halogen interactions among others [22]. Mo has just published a paper questioning whether the theory of atoms in molecules topological parameters can provide an effective measure of hydrogen bond strength [23].

* Tel.: +1 773 325 4343; fax: +1 773 325 7421.
E-mail address: rparra1@depaul.edu

2210-271X/$ - see front matter © 2012 Elsevier B.V. All rights reserved.
http://dx.doi.org/10.1016/j.comptc.2012.07.032

Another directional non-covalent interaction that has begun to receive a great deal of attention over the last two decades is the halogen bond interaction [24]. Although a recommended definition is yet to be released by the IUPAC Task Group, some researchers have already advanced insightful definitions of what a halogen bond is. For example, Legon [25] has suggested the following definition echoing that for the hydrogen bond definition given by the IUPAC Task Group: *The halogen bond is an attractive interaction between a halogen atom X from a molecule or fragment R—X in which R is a group more electronegative than X or is X itself, and an atom or a group of atoms A in the same molecule R—X or in a different molecule B, where there is evidence of bond formation.* A much shorter and thought-provoking definition has been given by Metrangolo et al. [26]: *Halogen bonding is the non-covalent interaction where halogen atoms function as electrophilic species.* Indeed, the notion that an atom surrounded by lone pairs is somehow able to accept additional electron density from other atoms is mind bugging. Not all halogens have the same ability to form halogen bonds, however, and even for the same halogen, the ability to form a halogen bond and the strength of the interaction depends on the atom or group to which it is covalently bonded. The halogen bond interaction has been explained in terms of the positive electrostatic potential that a covalently bonded halogen atom may develop in its outer side, opposite to the covalent bond and pointing toward any potential electron donor [27–29]. This region of positive electrostatic potential has been termed the σ-hole, and is responsible for the directional properties of the halogen bond. It has been found that the strength of a halogen bond increases with the halogen atoms's size (polarizability) and with the electron-withdrawing nature of the atom or group the halogen atom is covalently bound to, which increases the magnitude of the positive potential. The strength of a halogen bond follows the general trend F < Cl < Br < I. Fluorine atoms in common organic molecules usually show a little, if any, positive electrostatic potential, but they also might function as halogen bonding donors [30]. A definition that incorporates more explicitly the origin of the interaction has been proposed by Politzer et al. [31]: *A halogen bond is a highly directional, electrostatically-driven non-covalent interaction between a region of positive electrostatic potential on the outer side of the halogen X in a molecule R—X and a negative site B, such as a lone pair of a Lewis base or the π-electrons of an unsaturated system.*

The growing importance of the halogen bond is highlighted by recent review articles [24–35] and a book devoted to its fundamentals and applications [36]. The book and recent reviews demonstrate the explosive and ongoing growth in the number of publications concerned with the halogen bond. The halogen bond has found applications in a wide variety of fields including chemistry, biology, drug design, and materials science. Some authors have conducted systematic comparisons between the hydrogen bond and the halogen bond [37–41]. These studies demonstrate that the halogen bond and the hydrogen bond could compete and even interfere with each other, but the two interactions could also coexist and cooperate in building more complex and functional supra-molecular structures.

One area of fundamental interest is the possible non-additive or cooperative enhancement of intermolecular interactions like hydrogen and halogen bond interactions. It should be noted, however, that the number of studies on possible cooperative effects in halogen-bonded clusters is much smaller than the corresponding studies on hydrogen bonded clusters. Some recent studies on the cooperative effects in halogen bonds have been reported [42–48]. The primary purpose of the present study is to contribute to the growing overall understanding of the halogen bond. In particular, the strength of the N—X···N interactions for X = Cl, Br, or I (halogen bond) relative to that for X = H (hydrogen bond) is examined in formamidine and its mono-halogenated analogues chosen as convenient model systems for resonance-assisted X-bond interaction.

2. Computational details

Geometry optimizations and frequency calculations were carried out using the GAUSSIAN 09 program [49]. Except for the iodine atom, the calculations were performed with the Dunning's aug-cc-pVDZ correlated basis set [50,51]. To account for relativistic effects in the iodine-containing clusters, scalar-relativistic pseudopotentials along with the aug-cc-pVDZ-PP basis set were used for the iodine atom [52], and the aug-cc-pVDZ was used for the other atoms. Both the B3LYP [53–56] and M052X [57,58] density functional theory (DFT) methods were employed for geometry and frequency calculations. In a recent publication, Wang et al. examined the reliability of the M052X functional for halogen-bonded complexes and found it to perform on average quite well, even better than the B3LYP functional, against the MP2/aug-cc-pVTZ level of theory [59]. The calculated harmonic vibrational frequencies confirmed whether or not an optimized geometry corresponded to a minimum on the potential energy surface. Geometry optimizations were performed using the Opt = tight, and Int = Ultrafine options. The DFT optimized geometries were used as starting initial geometries for optimizations using the MP2 method and the same basis sets as those used with the DFT methods. Frequency calculations at the MP2 level were computed only for the MP2 optimized monomers and dimers. Interaction energies were computed at the same level of theory the geometries were obtained, and they were also corrected for basis set superposition error (BSSE) using the Boys–Bernardi counterpoise procedure [60]. The theory of atoms in molecules (AIM) of Bader [61] as implemented in the Gaussian 09 and the AIM2000 software package [62] was employed to analyze topological features of electron density of the MP2 optimized structures. Second order perturbation theory analysis of Fock Matrix in Natural Bond Order (NBO) basis were obtained for the various MP2 optimized molecular systems using the NBO program as implemented in the Gaussian 09 package [63–65]. Both AIM and NBO analyses were performed on B3LYP/aug-cc-pVDZ wavefunctions of minimum energy structures obtained with the same basis set at the MP2 level. Again, for the systems containing iodine atoms the aug-cc-pVDZ-PP basis set for I, and aug-cc-pVDZ basis set for the other atoms were used for the AIM and NBO calculations.

3. Results and discussion

3.1. Geometries

Selected MP2 optimized geometrical parameters of the HN═CHNHX (X = H, Cl, Br, or I) molecules in its *E* configuration are shown in Table 1. Fig. 1 shows the general shape of the molecule conveniently labelled to facilitate discussion. Selected geometrical parameters for MP2 optimized dimers and trimers are also listed in Table 1. The optimized parameters obtained with the DFT methods M052X and B3LYP are found in Tables 2 and 3 respectively. With regard to the monomers, both DFT methods predict fairly similar (within 0.006 Å) N═C, C—N, and N—H bond lengths. The corresponding MP2 bond lengths are longer (0.014–0.021 Å). The B3LYP nitrogen-halogen bond lengths are somewhat longer (0.026–0.031 Å) than the M052X values. The MP2 values lie in between those predicted by the two DFT methods. The extent of pyramidalization around nitrogen in the NHX group can be gauged by the dihedral angles τ_{XNHC}, and $\tau_{HN—CH}$. Accordingly, the pyramidal character on the NHX motif should decrease with increasing τ_{XNHC} values, and decreasing $\tau_{HN—CH}$ values. Both DFT methods produce very similar values for these dihedrals, but the MP2 results

Table 1
Selected geometrical parameters for HN=CHNHX clusters obtained at the MP2 level. Distances in Å, and angles in °.

X	N=C	C—N	N—X	τ_{XNHC}	τ_{HN-CH}	X···N	$\Theta_{N-X\cdots N}$	X···X
Monomers								
H	1.293	1.382	1.015	141.3	27.0			
Cl	1.285	1.401	1.743	129.4	41.7			
Br	1.286	1.398	1.884	130.8	40.0			
I	1.288	1.392	2.072	134.3	35.9			
Dimers								
Cyclic								
H	1.305	1.356	1.035	180.0	0.4	1.906	175.3	2.593
Cl	1.290	1.393	1.743	131.5	39.0	3.042	166.0	3.324
Br	1.294	1.387	1.885	134.7	35.0	3.011	162.2	3.417
I	1.300	1.375	2.073	143.8	25.7	3.064	156.8	3.627
Open								
I	1.296	1.380	2.086	141.3	27.7	2.755	177.0	3.890
	1.295	1.375	2.065	142.9	27.2	4.606	133.4	
Trimers								
C_3 symmetry								
H	1.304	1.355	1.020	177.5	0.0	1.976	152.8	3.415
Cl	1.290	1.391	1.746	132.3	36.4	2.855	169.9	3.741
Br	1.296	1.376	1.899	137.9	27.0	2.667	170.5	3.839
I	1.328	1.328	2.263	151.2	1.7	2.263	171.7	3.953
C_1 symmetry								
H	1.306	1.354	1.033	174.2	6.0	1.898	169.7	3.041
	1.302	1.360	1.028	156.9	12.2	1.989	156.0	3.045
	1.305	1.361	1.035	149.4	10.8	1.923	160.0	2.929
Average	1.304	1.359	1.032	160.2	9.7	1.937	161.9	3.005

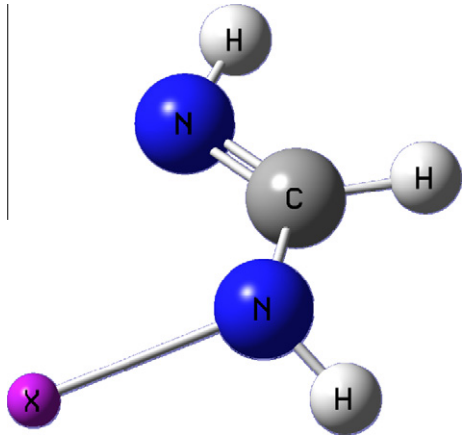

Fig. 1. Formamidine (X = H) and its mono-halogenated analogues (X = Cl, Br, or I) used to investigate intermolecular halogen and hydrogen bond interactions.

show τ_{XNHC} and τ_{HN-CH} values that are respectively smaller, and larger than their DFT counterparts. Nonetheless, based on these dihedral angles, all methods predict the following trend in the degree of pyramidalization for the various monomers: NHCl ≈ NHBr > NHI > NHH.

Initial guess geometries for the dimers studied here are based on a cyclic structure in which each molecule acts simultaneously as an X-bond donor and as an X-bond acceptor (X = H, Cl, Br, or I). Upon geometry optimization and frequency calculations, all methods agree that the cyclic structure is indeed a minimum for X = H, but a saddle point of first order (one imaginary frequency) for X = I. Fig. 2A shows the MP2 optimized dimer for X = H. A further geometry optimization with all methods for the dimers of X = I, using a guess geometry resulting from perturbing the molecule along the imaginary frequency, leads to a minimum-energy open structure with one molecule acting as the I-bond donor and the other as the I-bond acceptor. Figs. 2B and 2C show respectively the resulting cyclic and open dimers. For dimers for which X = Cl, or Br, both MP2 and M052X find the cyclic structures to be minimum energy structures, but in sharp contrast, B3LYP finds the cyclic structures for these dimers to be saddle points of first order, and the open structures to be the actual minimum energy structures. Interestingly, optimizing the B3LYP open structures (for X = Cl, Br) with either the M052X or the MP2 method results in the cyclic structures found originally with these methods.

With regard to intermolecular geometrical parameters, all theoretical models find the X···N distances to be much shorter than the sum of the van der Waals radii confirming that a sizeable attractive interaction is taking place. For the cyclic dimers, the linearity of the N—X···N interaction is largest for X = H (about 175°), but it undergoes a sizable reduction when X is a halogen. For example, at the MP2 level the reduction in the N—X···N angles are about 10°, 13°, and 19° for X = Cl, Br, and I respectively. The reduction in the N—X···N angle can be understood as the dimer trying to adopt a geometry that strikes a balance between the attractive halogen bond interaction, and the steric strain brought about by the proximity of two large halogen atoms in the cyclic dimers. All methods agree that the repulsive I···I interactions in the cyclic structure are too large to be overcome by the N—I···N interactions, and the dimer adopts rather a more open structure with an I···I distance much larger than that in the cyclic dimer. The most pronounced difference is given by the B3LYP method (0.372 Å), followed by M052X (0.297 Å), and then MP2 (0.263 Å). In general for X = halogen, the B3LYP results suggest that the steric X···X interactions are dominant irrespective of the halogen atom, and thus predict open structures. With only one halogen-bond interaction in the open dimers, the corresponding X···N distances are much shorter, and the N—X···N angle much wider than those in their cyclic dimer counterparts. Based on the intermolecular geometrical parameters, the strength of the N—X···N interaction in the minimum energy dimers follows the order N—H···N >

Table 2
Selected geometrical parameters for HN=CHNHX clusters obtained at the M052X level. Distances in Å, and angles in °.

X	N=C	C—N	N—X	τ_{XNHC}	τ_{HN-CH}	X···N	$\Theta_{N-X\cdots N}$	X···X
Monomers								
H	1.275	1.367	1.007	151.8	19.0			
Cl	1.266	1.386	1.720	135.1	36.5			
Br	1.266	1.385	1.872	134.3	36.2			
I	1.268	1.378	2.059	139.2	30.8			
Dimers								
Cyclic								
H	1.287	1.346	1.026	180.0	0.0	1.954	175.7	2.584
Cl	1.271	1.378	1.719	138.0	32.6	3.117	164.9	3.373
Br	1.273	1.374	1.869	139.4	30.9	3.131	161.5	3.481
I	1.282	1.358	2.060	155.7	16.4	3.084	156.7	3.612
Open								
I	1.277	1.364	2.073	149.4	20.8	2.797	177.1	3.908
	1.276	1.360	2.051	151.5	19.8	4.685	132.6	
Trimers								
C_3 symmetry								
H	1.286	1.345	1.020	180.0	0.0	2.047	150.6	3.384
Cl	1.269	1.375	1.720	139.8	31.3	2.931	163.4	4.346
Br	1.274	1.365	1.878	143.0	24.2	2.787	168.5	4.003
I	1.313	1.313	2.267	153.5	0.7	2.263	171.5	3.974
C_1 symmetry								
H	1.286	1.349	1.024	158.8	6.3	1.998	158.5	3.169
	1.287	1.345	1.023	179.6	2.3	1.972	164.3	3.058
	1.284	1.347	1.019	168.8	5.8	2.067	150.8	3.029
Average	1.286	1.347	1.022	168.9	4.8	2.013	157.8	3.082

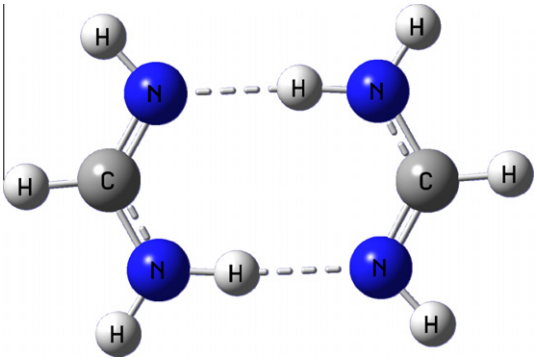

Fig. 2A. MP2 minimum energy structure of formamidine cyclic dimer.

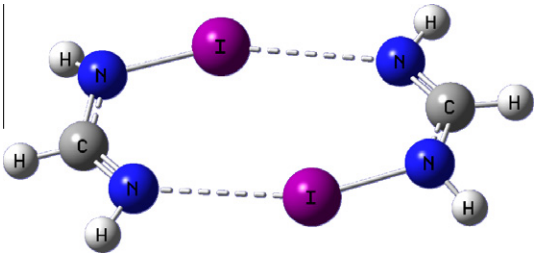

Fig. 2B. MP2 optimized mono-iodinated formamidine cyclic dimer. The cyclic structure is a first-order saddle point at all levels of theory: MP2 (v_i = 31 cm^{-1}), M052X (v_i = 40 cm^{-1}), and B3LYP (v_i = 40 cm^{-1}).

N—I···N > N—Br···N > N—Cl···N. For example, at the MP2 level the reduction of the X···N distances with respect to the sum of the van der Waals radii are estimated to be 31% (X = H) > 26% (X = I) > 14% (X = Br) > 9% (X = Cl).

Dimerization also brings about changes in the intramolecular geometrical parameters of the constituent monomers, and the

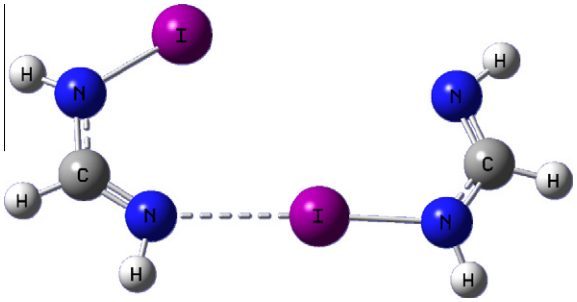

Fig. 2C. MP2 minimum-energy structure of mono-iodinated formamidine dimer.

extent to which these changes occur in the various systems is expected to reveal the relative strength of the corresponding N—X···N interactions. The results from all theoretical methods show similar percentage changes in the intramolecular parameters. Close examination of the changes brought about by dimerization reveals the importance of the N=C—N—X π-conjugated system in strengthening the N—X···N interaction. This is evinced by elongation of the N=C bond and contraction of the C—N bond. An elongation of the donor N—X bond is seen in the open dimer structures, and in the cyclic dimer for X=H. The N—X bond changes little upon cyclic dimerization for X = halogen which seems reasonable as an elongation of this bond would likely increase the steric X···X interaction. The largest geometric changes upon dimerization are the decrease of τ_{HN-CH} and the increase of τ_{XNHC} signalling a reduction in the pyramidal character on the NHX motif. For example, the large increase in τ_{HNHC} and decrease in τ_{HN-CH} obtained with all methods results in complete planarization on the nitrogen centre in the NHH group. The increased planarity on the NHX group enhances the polarization of the π-conjugated system, which in turn strengthens the N—X···N interaction. The calculated changes in the intramolecular geometrical parameters suggest the following ranking in the interaction strength:

Table 3
Selected geometrical parameters for HN=CHNHX clusters obtained at the B3LYP level. Distances in Å, and angles in °.

X	N=C	C—N	N—X	τ_{XNHC}	τ_{HN-CH}	X···N	$\Theta_{N-X\cdots N}$	X···X
Monomers								
H	1.281	1.372	1.012	151.0	19.8			
Cl	1.271	1.391	1.748	134.5	37.1			
Br	1.272	1.387	1.898	135.7	35.5			
I	1.275	1.380	2.090	140.0	30.8			
Dimers								
Cyclic								
H	1.294	1.350	1.036	180.0	0.0	1.908	174.6	2.602
Cl	1.276	1.383	1.744	137.6	33.7	3.241	163.9	3.472
Br	1.280	1.376	1.894	141.4	29.5	3.151	160.3	3.535
I	1.287	1.365	2.089	152.6	19.2	3.188	155.5	3.716
Open								
I	1.282	1.368	2.106	149.3	21.6	2.804	173.9	4.088
	1.282	1.364	2.079	151.3	20.6	5.116	127.0	
Cl	1.275	1.384	1.749	137.6	33.5	2.977	175.3	3.789
	1.273	1.385	1.743	136.8	34.9	4.550	142.9	
Br	1.277	1.378	1.904	140.3	30.1	2.858	175.4	3.845
	1.276	1.377	1.890	140.3	30.9	4.671	137.1	
Trimers								
C_3 symmetry								
H	1.293	1.352	1.029	179.8	0.0	1.983	153.3	3.419
Cl	1.276	1.379	1.747	139.8	31.2	2.942	165.5	4.403
Br	1.287	1.357	1.914	150.4	17.0	2.619	168.8	4.134
I	1.319	1.319	2.293	161.5	0.7	2.293	170.3	4.153
C_1 symmetry								
H	1.292	1.350	1.030	172.1	0.2	1.976	156.2	3.312
	1.293	1.352	1.030	163.5	5.2	1.980	155.9	3.337
	1.294	1.349	1.031	175.0	4.2	1.953	158.2	3.265
Average	1.293	1.350	1.030	170.2	3.2	1.970	156.7	3.305

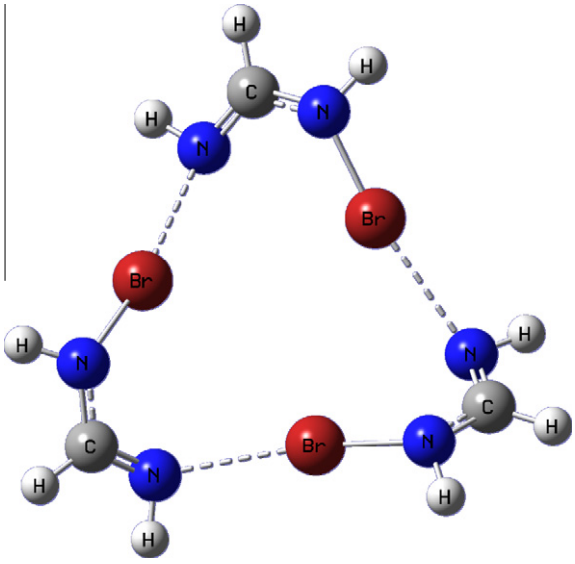

Fig. 3A. MP2 optimized geometry of the mono-brominated formamidine cyclic trimer with symmetry C_3. Similar in shape are the corresponding geometries for the trimers of mono-chlorinated formamidine, and formamidine. It should be noted, however, that the symmetric cyclic trimer of formamidine is found to be a first-order saddle point with the DFT methods: M052X ($v_i = 22\ cm^{-1}$) and B3LYP ($v_i = 15\ cm^{-1}$). No frequency calculations were performed at the MP2 level.

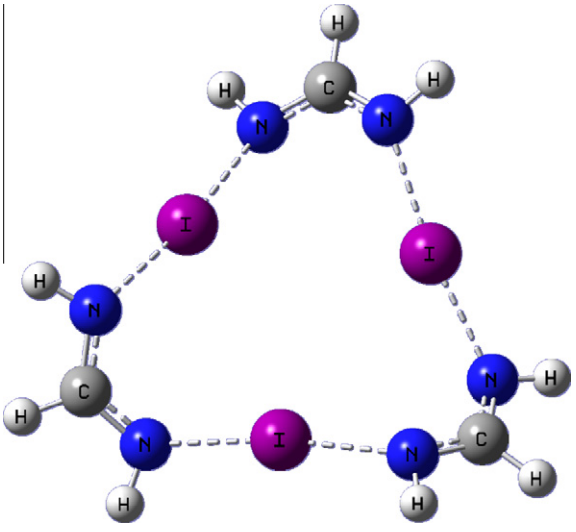

Fig. 3B. MP2 optimized geometry of the mono-iodinated formamidine cyclic trimer with symmetry C_3.

N—H···N > N—I···N > N—Br···N > N—Cl···N. The ranking mirrors that obtained previously based on the intermolecular parameters.

It is of interest to examine whether the above ranking of the N—X···N strength remains with clusters of larger size. To that end, trimers were optimized using cyclic structures. It was expected that while the small size of the H atom would enable strong H-bond interactions in the dimer with short and linear N—H···N interactions, this same fact would weaken the H-bond interactions upon trimerization due to the geometrical constrains required for planar or quasi-planar cyclization. The opposite was expected to be true for trimer formation of the halogen-bonded structures. In particular, trimer formation should increase the X···X distance which for the large halogen atoms would mean an important decrease in steric repulsions. M052X and B3LYP optimi-

zation of the symmetric halogen-bonded trimers resulted in minimum energy structures of C_3 symmetry. The symmetric H-bonded trimer (X=H) was found to be a saddle point of first order at the B3LYP ($\nu_i = 15\ cm^{-1}$), and at the M052X level ($\nu_i = 22\ cm^{-1}$). For any given trimer, further optimization at the MP2 level using as initial guess the optimized geometry of either DFT method resulted in the same structure whose overall shape is exemplified by that of the trimer of mono-bromo formamidine shown in Fig. 3A. Relevant structural parameters are listed in Tables 1 (MP2), 2 (M052X), and 3 (B3LYP).

All theoretical methods predicted a severe deviation from linearity of the N—H···N bond, which according to Table 1 amounts to 22.5° reduction relative to the cyclic dimer. Another striking feature, upon formation of the symmetric H-bonded trimer, is the significant elongation of the N—H···N intermolecular distance, accompanied by the also significant shortening of the covalent N—H distance. At the MP2 level, for example, the N—H···N distance is larger by 0.070 Å, and the N—H bond shorter by 0.015 Å, with similar results from the DFT geometries (Tables 2 and 3). All these geometrical changes show that formation of the symmetric trimer weakens the H-bond interaction relative to the H-bonded dimer. All methods consistently showed that the deviation from linearity in the halogen-bonded trimers is less than that in the hydrogen-bonded trimer. Relative to the respective cyclic dimers, the increase in the N—X···N angle follows the order N—I···N > N—Br···N > N—Cl···N. For the open dimers, however, the N—X···N angles are actually larger. Trimer formation for the halogen-bonded systems also results in very important reductions in both the N—X···N and the X···X intermolecular distances. The changes in these geometrical parameters, and in fact in all the parameters listed in Table 1, indicate that the halogen-bond interaction is stronger in the trimers than in the corresponding dimers, a result contrary to what was noted for the H-bond interaction. Clearly the most striking geometrical changes upon trimer formation happen for the N—I···N interaction. Indeed, the strengthening of the interaction is so dramatic that iodine is now symmetrically located between the two nitrogen atoms as N···I···N as shown in Fig. 3B. The effective detachment of the iodine atom causes the rest of the molecule to adopt an essentially planar geometry with a close to zero τ_{HN-CH} angle, and identical carbon-nitrogen bond lengths. Such an abrupt change in bonding pattern can only be generated by especially strong-enough interactions capable of overcoming the large energy required to produce the geometrical deformation of the constituent monomers in the trimer. To the best of the author's knowledge, the symmetric N···I···N interaction found in this work is the first reported for a neutral halogen-bonded trimer cluster in the gas phase. This finding complements that by Carlsson et al. who very recently reported experimental evidence confirming the existence of symmetric $[N\cdots I\cdots N]^+$ interactions both in solution and in the crystal [66,67]. The authors used model systems containing two pyridine-type Lewis bases to bind an electropositive iodine or bromine. The authors discovered that symmetric $[N\cdots Br\cdots N]^+$ also exists in solution. The experimental results were supported by B3LYP calculations. Interestingly, the calculated $[N\cdots I\cdots N]^+$ distances of 2.301 Å are very close to the values obtained in this work for the neutral clusters: 2.293 Å at the B3LYP level, and 2.263 Å at both the M052X and MP2 levels.

In an effort to find a minimum energy structure for the H-bonded trimer, further geometry optimizations were performed with the two DFT methods using an initial guess geometry resulting from perturbing the molecule along the pertinent imaginary frequency found in the symmetric trimer. Both methods yielded optimized geometries that are indeed minimum energy structures (no imaginary frequencies). The structural parameters are summarized in Tables 2 (M052X), and 3 (B3LYP). Optimization at the MP2 level using the optimized geometry of either DFT method converged to the same structure of symmetry C_1, and is shown in Fig. 4, with relevant geometrical parameters listed in Table 1. All theoretical methods agree with the overall shape of the trimer. The methods also show consistently that the three H-bonded interactions in the minimum energy trimer are no longer identical, and that even this structure exhibits a sizeable decrease in the strength of the H-bond interaction relative to the cyclic dimer. The weakening effect is not as pronounced as in the symmetric, C_3, cyclic trimer, however. For example, at the MP2 level the average H-bond distance in the trimer of C_1 symmetry is shorter by about 0.040 Å, and the N—H···N angle is wider by about 9° than in the trimer of C_3 symmetry. Moreover, the monomers in the minimum energy trimer also show, an average, a pyramidal structure on the NHH centre with τ_{XNHC}, and τ_{HN-CH} values that are respectively about 18° smaller and 10° larger than those in the more symmetric trimer.

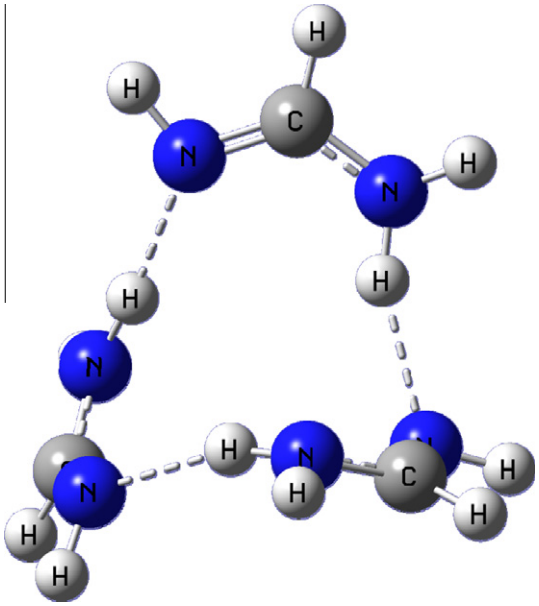

Fig. 4. MP2 optimized geometry of the mono-chlorinated formamidine cyclic trimer with symmetry C_1. The C_1 cyclic trimer of formamidine is found to be a minimum energy structure (no imaginary frequencies) with the DFT methods M052X and B3LYP.

3.2. N—X vibrational frequency shift

Changes in the strength of the N—X···N interaction upon trimer formation should also manifest in the frequency shift of the N—X stretching donor in the trimer and the dimer. The calculated harmonic frequencies of the N—X stretching mode associated with the N—X donor in each dimer and trimer complex are listed in Table 4. As expected, the weakening of the H-bond interaction is manifested in a large blue shift in the N—H stretching frequency, regardless of the method used. In contrast, an equally sizeable red shift in the donor N—I stretching frequency reveals a major strengthening of the N—I···N interaction upon trimerization. For the other two halogens, the frequency shifts to the red, although rather small, do indicate the cooperative strengthening of the N—X···N interactions in the corresponding the trimers.

3.3. Energetics

The average energy of interactions, defined as the interaction energy divided by the number of N—X···N interactions in the cluster, are listed in Table 5 for each one of the optimized dimer and trimer structures. The interaction energies were obtained as the

Table 4
N—X stretching frequencies (cm^{-1}) of the N—X donor calculated with the M052X and B3LYP methods.

X	Cyclic dimer	C_3 Trimer	Open dimer	C_1 Trimer
M052X				
H	3326	3467		3448
	3273	3435		3349
		3407		3324
Cl	676	670		
	671	665		
		665		
Br	590	580		
	586	580		
		579		
I	536	369	519	
	531	318		
		318		
B3LYP				
H	3193	3307		3291
	3132	3307		3280
		3275		3247
Cl	638	636	628	
	635	630		
		630		
Br	560	531	548	
	557	530		
		527		
I	500	335	490	
	498	300		
		298		

difference between the energy of the cluster and the sum of the energies of the constituent monomers, assuming they have the same geometries as in the corresponding dimers or trimers. All interaction energies were corrected for basis set superposition error (BSSE). Also listed in Table 5 are the average complexation energies of the clusters which take into account the increase in energy of the monomers in the clusters due to the geometrical deformations that each monomer suffers upon cluster formation. Thus, the difference between complexation and interaction energies indicates the extent to which cluster formation perturbed the geometry of the constituent monomers relative to their geometries when they are isolated and fully relaxed or optimized. In particular, the results for the formamidine dimer listed in Table 5 are in accord with the high-level ab intio results reported by Šponer and Hobza [68].

Based on either the average interaction energies or average complexation energies, The MP2 method and the two DFT methods agree on the following interaction strength sequence in the dimers: N—H···N > N—I···N > N—Br···N > N—Cl···N. It is worth noting that the M052X results are generally close to those obtained using the MP2 method. The major difference occurs for the N—I···N dimer interactions which tend to be overestimated with the M052X method. The B3LYP energetic results of the H-bonded dimer are fairly close to those given by the other two methods. However, the B3LYP results for the halogen-bonded dimer structures are substantially higher (smaller in magnitude) than those predicted by the other two methods.

Table 5 shows that trimerization destabilizes the H-bond interaction as seen in a decrease of about 8% in the magnitude of the average H-bond interaction energy regardless of the theoretical method used. A similar reduction of about 13% is seen for the average complexation energy upon trimer formation of the N—H···N interactions. Interestingly, the average interaction energies of the two different trimers of the N—H···N interactions are very similar, although it should be recalled that the trimer with C_3 symmetry is not a minimum but a saddle point of first order. For the halogen-bonded systems, on the other hand, trimerization produces a very important increase in the magnitude of the average interaction energies. For example, the MP2 average interaction energy for the N—Cl···N interactions in the trimer increases by a factor of 1.28 when compared with that in the dimer. The corresponding cooperative increase for the N—Br···N interaction is 1.98. The largest and most dramatic change is seen for the N—I···N interaction which is found to increase by a factor of 3.36, when compared with that in the open dimer. The increase factors calculated with the two DFT methods are fairly similar to those found with the MP2 method, except for the B3LYP increase factor of 4.55 for the N—I···N interaction. This factor is much larger than those obtained with the MP2 (3.36) and M052X (3.39) method. As a reference, Carlsson et al. reported electronic binding energies for the symmetric $[N\cdots I\cdots N]^+$ interactions in the two model systems employed, at the B3LYP level and using the PCM method with CD_2Cl_2 as solvent, that correspond to average values of about 20.0 kcal/mol and 17.3 kcal/mol [67]. These values, although smaller, compare well with those found for the trimer clusters studied here.

The increase factors for the complexation energies of the N—Cl···N, and N—Br···N are somewhat comparable to those for the corresponding interaction energies. A dramatic reduction in the increase factor is found for the N—I···N complexation energies. For example, while the MP2 average interaction energy in the trimer is 3.36 times that found in the open dimer, the respective average complexation energy is 1.35 times that of the open dimer. This reduction in the increase factor can be traced down to the very large deformation energy that each monomer in the trimer undergoes, when compared with that upon dimer formation. At the MP2 level, for example, while dimer formation increases the energy of each monomer due to deformation by 0.43 kcal/mol, trimer formation raises the energy of a monomer by 14.84 kcal/mol. Such large deformation energy is not observed in the other two halogen-bonded systems; indeed the deformation energies in these trimers are comparable to those of their dimers.

3.4. AIM and NBO

The strength of the various N—X···N interactions was also studied by analyzing some relevant topological parameters of the

Table 5
Average interaction energies, ΔE^{int}, and average complexation energies, ΔE^{comp}, in kcal/mol.[a]

X	ΔE^{int}			ΔE^{comp}		
	MP2	M052X	B3LYP	MP2	M052X	B3LYP
Cyclic dimer						
H	−7.47	−7.41	−7.19	−6.46	−6.75	−6.34
Cl	−1.75	−1.77	−0.35	−1.67	−1.71	−0.27
Br	−2.59	−2.44	−1.08	−2.37	−2.27	−0.90
I	−3.28	−4.17	−1.93	−2.69	−3.45	−1.42
Open dimer						
I	−7.13	−8.20	−5.52	−6.73	−7.77	−5.09
Cl			−0.77			−0.70
Br			−2.64			−2.53
C_3 Trimer						
H	−6.87	−6.74	−6.58	−5.64	−5.87	−5.44
Cl	−2.24	−1.96	−0.87	−2.10	−1.89	−0.69
Br	−5.13	−4.58	−4.84	−3.90	−4.04	−3.28
I	−23.94	−27.82	−25.14	−9.11	−11.81	−10.54
C_1 Trimer						
H	−6.90	−6.83	−6.64	−5.89	−6.03	−5.56

[a] Average ΔE^{int} refers to the BSSE-corrected interaction energy divided by the number of N—X···N interactions in the cluster, assuming that each isolated monomer has the same geometry as that in the complex. Average ΔE^{Comp} takes into account the increase in energy of the monomers in the clusters due to the geometrical deformations that each monomer suffers upon cluster formation.

Table 6
MP2 average interaction energies, ΔE^{Int}, and B3LYP average $n_N \rightarrow \sigma^*$N—X delocalization energies, $E^{(2)}$ in kcal/mol. B3LYP topological parameters in 10^{-2} au. Properties calculated for the MP2 minima.

X	ΔE^{Int}	$E^{(2)}$	ρ_c	H_c	$-V_c/G_C$
Dimer					
Cyclic					
H	−7.47	20.61	3.305	−0.221	1.10
Cl	−1.75	2.01	1.099	0.151	0.80
Br	−2.59	4.07	1.405	0.124	0.87
Open					
I	−7.13	15.66	2.760	−0.566	1.55
Trimer					
C_3 Symmetry					
Cl	−2.24	2.92	1.533	0.166	0.86
Br	−5.13	10.60	2.679	−0.004	1.00
I	−23.94	106.40	7.650	−3.645	1.80
C_1 Symmetry					
H	−6.90	15.61	2.929	−0.086	1.04

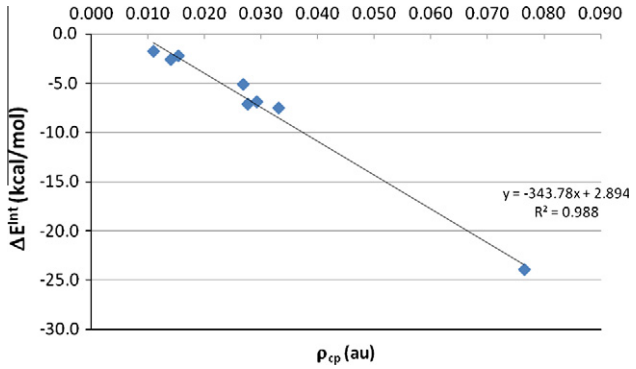

Fig. 5. Linear correlation between the magnitude of the average interaction energies and the electron charge density at the X···N critical point, ρ_{cp}.

electron densities at the hydrogen bond (X = H) or halogen-bond (X = Cl, Br, or I) critical points through the theory of atoms in molecules, AIM, of Bader [61]. The results for the MP2 minimum energy dimers and trimers are shown in Table 6, along with the average interaction energies. Inspection of Table 6 reveals that the magnitude of the electron density calculated at the N—X···N bond critical point, ρ_c, correlates with the calculated interaction energies. The fairly linear correlation is better appreciated in Fig. 5. The good correlation between ρ_c and the hydrogen bond or the halogen bond strength has been pointed out by others [69–72]. Previous studies have also suggested that the sign of the total electron energy density at the bond critical point, H_c, reveals the nature of the interaction as partly covalent ($H_c < 0$), or non-covalent ($H_c > 0$). The ratio $-G_C/V_c$, where G_C and V_c represent the kinetic and potential energy densities at the critical point, has also been used to indicate the nature of an interaction [19]. Thus, a partly covalent interaction is said to exist if this ratio is between 1 and 2, while a weak closed-shell interaction is said to exist if the ratio if smaller than 1. A covalent interaction is found to correspond with $-G_C/V_c > 2$. From Table 6, it is apparent that both H_c and $-G_C/V_c$, consistently show that partially covalent N—X···N interactions exist for the dimers when X = H or I, but closed-shell interactions exists when X = Cl or Br. The covalent character when X = I appears more pronounced than that when X = H. Trimer formation lowers somewhat the covalent character of the N—H···N interaction, but heightens dramatically the covalent character for the N—I···N interaction. The cooperative strengthening of the N—Br···N interaction upon trimerization is seen to result in a

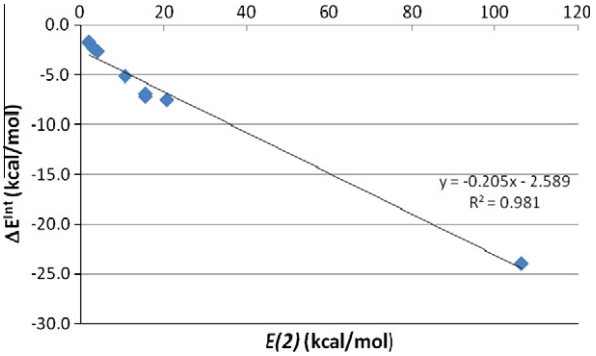

Fig. 6. Linear correlation between the magnitude of the average interaction energies and the average $n_N \rightarrow \sigma^*$N—X delocalization energies $E^{(2)}$.

partly covalent character for this interaction. Although the N—Cl···N interaction gains strength in the trimer, it remains a weak closed-shell interaction.

Additionally, the Natural Bond Orbital (NBO) analysis was performed to obtain the stabilization energy by second order perturbation theory, $E^{(2)}$. The NBO focus is on the stabilization energy resulting from interactions between the filled lone-pair orbital of the nitrogen acting as X-bond acceptor, and the empty anti-bonding orbital of the halogen-bond donor N—X: $n_N \rightarrow \sigma^*_{N-X}$. The results for the MP2 minimum energy dimers and trimers are also shown in Table 6. Inspection of Table 6 makes apparent that the delocalization energy $E^{(2)}$ is largest for the formamidine dimer, followed by its mono-iodinated dimer analogue. Trimer formation brings about a small reduction in $E^{(2)}$ for formamidine consisting with the weakening of the N—H···N interaction as demonstrated already through geometrical, vibrational, energetic, and topological parameters. In general, the calculated delocalization energies correlate fairly linearly with the interaction energies as seen in Fig. 6. The small gain in the N—Cl···N strength seen in the trimer is revealed by the also small increase in the delocalization energy. The enhancement in the delocalization energy for the N—Br···N is important as it more than doubles that of the dimer. However, the most substantial increase in the $E^{(2)}$ upon trimerization is seen for the N—I···N interaction. Such a substantial increase in the delocalization energy is connected with an equally substantial increase in the population of the anti-bonding σ^*_{N-I} orbital and hence with the weakening and elongation (rupture) of the N—I covalent bond.

3.5. Effects of enlarging the basis set

The use of higher correlation methods and larger basis sets on the calculated properties of the systems investigated here is certainly a subject of future work. For now, the effects of enlarging the basis set to aug-cc-pVTZ on the properties of the weakest dimer interaction, namely the monochlorinated formamidine dimer, was examined with all three theoretical methods used in this work, and the results are summarized in Table 7. In particular, it is seen that with the aug-cc-pVTZ both the MP2 and M052X find the cyclic dimer structure to be a minimum energy structure, while the B3LYP method finds that the open dimer is the minimum energy structure. This is the same result observed with the smaller aug-cc-pVDZ basis set. Also as seen with the smaller basis set, optimizing the open dimer using the MP2 or M052X results in the cyclic structure. That is, no open dimer structure is found as a minimum energy structure with these two methods. The magnitudes of the interaction and complexation energies are found to increase by 0.35 kcal/mol at the MP2 level. There is also a small reduction (~0.01 Å) in the Cl···N distance, and an increase (~0.08 Å) in the Cl···Cl distance. The use of the larger basis set results in a small in-

Table 7
Effects of enlarging the basis set on calculated properties for HN═CHNHCl Dimer. Distances in Å, angles in °, energies in kcal/mol.

Cyclic dimer	MP2		M052X		B3LYP	
	aug-cc-pVDZ	aug-cc-pVTZ	aug-cc-pVDZ	aug-cc-pVTZ	aug-cc-pVDZ	aug-cc-pVTZ
Cl···N	3.042	3.028	3.117	3.137	3.241	3.301
$\Theta_{N-Cl\cdots N}$	166.0	165.7	164.9	164.8	163.9	163.7
Cl···Cl	3.324	3.302	3.373	3.377	3.472	3.502
ΔE^{Int}	−1.75	−2.12	−1.77	−1.70	−0.35	−0.40
ΔE^{Comp}	−1.67	−2.02	−1.71	−1.64	−0.27	−0.33

B3LYP

Open dimer	aug-cc-pVDZ	aug-cc-pVTZ
Cl···N	2.977	3.012
$\Theta_{N-Cl\cdots N}$	175.3	175.8
Cl···Cl	3.789	3.757
ΔE^{Int}	−0.770	−0.46
ΔE^{Comp}	−0.700	−0.41

[a]Average ΔE^{Int} refers to the BSSE-corrected interaction energy divided by the number of N—X···N interactions in the cluster, assuming that each isolated monomer has the same geometry as that in the complex. Average ΔE^{Comp} takes into account the increase in energy of the monomers in the clusters due to the geometrical deformations that each monomer suffers upon cluster formation.

crease in the Cl···N distance, but it has little effect on the interaction and complexation energies calculated with the two DFT methods and the smaller basis set for the cyclic dimer. As for the open dimer, the use of the larger bais set results in lengthening of the Cl···N distance, and in a relatively important reduction of the interaction and complexation energies. Indeed, the interaction and complexation energies for the open dimer are very close to those of the cyclic dimer with the larger basis set.

3.6. Summary and future work

The results of the computational study on the intermolecular N—X···N interaction occurring in dimer and trimer clusters of formamidine (X = H), and its mono-halogenated analogues (X = Cl, Br, or I) show that the hydrogen bond interaction is consistently stronger than the halogen bond interaction when the halogen is either Cl or Br. Trimerization strengthens the halogen bond interactions but weakens the hydrogen bond interaction. Despite these opposite effects, the hydrogen bond remains stronger than the halogen bond, when the halogen is Cl or Br. With regard to X = I, it is found that the N—I···N interaction is of comparable strength to the N—H···N interaction for the dimer clusters. Upon trimerization, however, the N—I···N interaction becomes much stronger than the N—H···N interaction. In fact, the iodine bond interaction in the trimer becomes so strong that it results in the iodine atom being symmetrically positioned between the two nitrogen atoms: N···I···N. Such a drastic geometrical change appears to be facilitated by the iodine being much larger and polarizable than the other X atoms. Certainly the size of the iodine atom gives it a better capacity to support the extent of positive charge developed upon separation from the nitrogen to which it is covalently bound. Likewise, the rest of the molecule needs to take care of the negative charge developed upon iodine separation. Here, the N═C—N fragment is instrumental in stabilizing the partial negative charge by delocalization through the π-conjugated system.

It remains a subject of future work to investigate whether other resonance-assisted halogen (particularly iodine) bonds exhibit the sort of symmetric N···X···N interactions observed in the model systems investigated in this work. It is also of great interest to investigate the metal ion binding abilities of the halogen-bonded trimers. Here the idea is to exploit the dual role that a halogen atom in the N—X···N interaction can play: in one role, the halogen atom is involved in a quasi-linear halogen bonding interaction through its σ-hole; in the other role, the halogen atom can interact with electrophiles, such as metal ions, through the negative electrostatic potential belt in the halogen atom that surrounds its σ-hole. The cyclic halogen-bonded trimers provide a cavity rich in electron density where a metal ion of suitable size can fit and be bound to the cluster. Research in this area is currently underway in the author's lab. This is an interesting and stimulating challenge both for theoretical and experimental work.

Acknowledgement

The author is grateful to the Department of Chemistry at DePaul University for its constant support.

References

[1] E.R. Johnson, S. Keinan, P. Mori-Sanchez, J. Contreras-Garcia, A.J. Cohen, W. Yang, Revealing noncovalent interactions, J. Am. Chem. Soc. 6498 (2010) 132.
[2] P. Hobza, K. Müller-Dethlefs, Non-covalent Interactions: Theory and Experiment. RSC Theoretical and Computational Chemistry Series No. 2, 2009.
[3] K. Müller-Dethlefs, P. Hobza, Non-covalent interactions: a challenge for experiment and theory, Chem. Rev. 143 (2000) 100.
[4] J.W. Steed, J.L. Atwood, Supramolecular Chemistry, second ed., Wiley, 2009.
[5] W.M. Latimer, W.H. Rodebush, Polarity and ionization from the standpoint of the Lewis theory of valence, J. Am. Chem. Soc. 1419 (1920) 42.
[6] P. Gilli, G. Gilli, The Nature of the Hydrogen Bond, Oxford University Press, Oxford, 2009.
[7] S.J. Grabowski (Ed.), Hydrogen Bonding: New Insights, Springer, Dordrecht, 2006.
[8] G.R. Desiraju, T. Steiner, The Weak Hydrogen Bond, Oxford University Press, Oxford, 1999.
[9] S. Scheiner, Hydrogen Bonding: A Theoretical Perspective, Oxford University Press, Oxford, 1997.
[10] G.A. Jeffrey, An Introduction to Hydrogen Bonding, Oxford University Press, Oxford, 1997.
[11] D.W. Bolen, G.D. Rose, Structure and energetics of the hydrogen-bonded backbone in protein folding, Annu. Rev. Biochem. 77 (2008) 339.
[12] T. Steiner, The whole palette of hydrogen bonds, Angew. Chem. Int. Ed. 48 (2002) 41.
[13] C.B. Aakeroy, A.M. Beatty, Solid state, crystal engineering and hydrogen bonds, ChemInform 679 (2004) 35.
[14] M. Meot-Ner, The ionic hydrogen bond, Chem. Rev. 213 (2005) 105.
[15] P. Hobza, Z. Havlas, Blue-shifting hydrogen bonds, Chem. Rev. 4253 (2000) 100.
[16] A. Barnes, Blue-shifting hydrogen bonds? Are they improper or proper?, J Mol. Struct. 3 (2004) 704.
[17] I. Akorta, I. Rozas, J. Elguero, Non-conventional hydrogen bonds, Chem. Soc. Rev. 163 (1998) 27.
[18] O. Takahashi, Y. Kohno, M. Nishio, Relevance of weak hydrogen bonds in the conformation of organic compounds and bioconjugates: evidence from recent experimental data and high-level *ab Initio* MO calculations, Chem. Rev. 6049 (2010) 110.
[19] S.J. Grabowski, What is the covalency of hydrogen bonding?, Chem Rev. 2597 (2011) 111.

[20] E. Arunan, G.R. Desiraju, R.A. Klein, J. Sadlej, S. Scheiner, I. Alkorta, D.C. Clary, R.H. Crabtree, J.J. Dannenberg, P. Hobza, H.G. Kjaergaard, A.C. Legon, B. Mennucci, D.J. Nesbitt, Defining the hydrogen bond: an account, Pure Appl. Chem. 1619 (2011) 83.
[21] E. Arunan, G.R. Desiraju, R.A. Klein, J. Sadlej, S. Scheiner, I. Alkorta, D.C. Clary, R.H. Crabtree, J.J. Dannenberg, P. Hobza, H.G. Kjaergaard, A.C. Legon, B. Mennucci, D.J. Nesbitt, Definition of the hydrogen bond, Pure Appl. Chem. 1637 (2011) 83.
[22] G. Sánchez-Sanz, C. Trujillo, I. Alkorta, J. Elguero, Electron density shift description of non-bonding intramolecular interactions, COMPTC 991 (2012) 124.
[23] Y. Mo, Can QTAIM topological parameters be a measure of hydrogen bonding strength? J. Phys. Chem. A, DOI: 10.1021/jp3029769.
[24] O. Hassel, Science 497 (1970) 170.
[25] A.C. Legon, The halogen bond: an interim perspective, Phys. Chem. Chem. Phys. 7736 (2010) 12.
[26] P. Metrangolo, F. Meyer, T. Pilati, G. Resnati, G. Terraneo, Halogen bonding in supramolecular chemistry, Angew. Chem. Int. Ed. 6114 (2008) 47.
[27] P. Politzer, P. Lane, M.C. Concha, Y. Ma, J.S. Murray, An overview of halogen bonding, J. Mol. Model. 305 (2007) 13.
[28] T. Clark, M. Hennemann, J.S. Murray, P. Politzer, Halogen bonding: the σ-hole, J. Mol. Model. 291 (2007) 13.
[29] P. Politzer, J.S. Murray, P. Lane, σ-Hole bonding and hydrogen bonding: competitive interactions, Int. J. Quantum Chem. 3046 (2007) 107.
[30] A.G. Dikundwar, T.N. Guru Row, Evidence for the "Amphoteric" nature of fluorine in halogen bonds: an instance of Cl···F contact, Cryst. Growth Des. 1713 (2012) 12.
[31] P. Politzer, J.S. Murray, T. Clark, Halogen bonding: an electrostatically-driven highly directional noncovalent interaction, Phys. Chem. Chem. Phys. 7748 (2010) 12.
[32] G. Cavallo, P. Metrangolo, T. Pilati, G. Resnati, M. Sansotera, G. Terraneo, Halogen bonding: a general route in anion recognition and coordination, Chem. Soc. Rev. 3772 (2010) 39.
[33] P. Auffinger, F.A. Hays, E. Westhof, P. Shing Ho, Halogen bonding in biological molecules, Proc. Natl. Acad. Sci. USA 16789 (2004) 101.
[34] R. Bertani, P. Sgarbossa, A. Venzo, F. Lelj, M. Amatic, G. Resnatid, T. Pilati, P. Metrangolo, G. Terraneo, Halogen bonding in metal–organic–supramolecular networks, Coord. Chem. Rev. 677 (2010) 254.
[35] E. Parisini, P. Metrangolo, T. Pilati, G. Resnati, G. Terraneo, Halogen bonding in halocarbon–protein complexes: a structural survey, Chem. Soc. Rev. 2267 (2011) 40.
[36] P. Metrangolo, G. Resnati (Eds.), Halogen Bonding: Fundamentals and Applications, Springer, Berlin, 2008.
[37] P. Metrangolo, H. Neukirch, T. Pilati, G. Resnati, Halogen bonding based recognition processes: a world parallel to hydrogen bonding, Acc. Chem. Res. 386 (2005) 38.
[38] E. Corradi, S.V. Meille, M.T. Messina, P. Metrangolo, G. Resnati, Halogen bonding versus hydrogen bonding in driving self-assembly processes, Angew. Chem. Int. Ed. 1782 (2000) 39.
[39] P. Metrangolo, G. Resnati, Halogens versus hydrogen, Science 918 (2008) 321.
[40] A.R. Voth, F.A. Hays, P. Shing Ho, Directing macromolecular conformation through halogen bonds, Proc Natl Acad Sci USA 6188 (2007) 104.
[41] W. Wang, Y. Zhang, B. Ji, On the difference of the properties between the blue-shifting halogen bond and the blue-shifting hydrogen bond, J. Phys. Chem. A 7257 (2010) 114.
[42] M.D. Esrafili, N.L. Hadipour, Characteristics and nature of halogen bonds in linear clusters of NCX (X = Cl and Br): an ab initio, NBO, and QTAIM study, Mol. Phys. 2451 (2011) 109.
[43] I. Alkorta, F. Blanco, J. Elguero, A computational study of the cooperativity in clusters of interhalogen derivatives, Struct. Chem. 63 (2009) 20.
[44] S.J. Grabowski, E. Bilewicz, Cooperativity halogen bonding effect – Ab initio calculations on $H_2CO\cdots(ClF)_n$ complexes, Chem. Phys. Lett. 427 (2006) 51.
[45] E. Bilewicz, A.J. Rybarczyk-Pirek, A.T. Dubis, S.J. Grabowski, Halogen bonding in crystal structure of 1-methylpyrrol-2-yl trichloromethyl ketone, J. Mol. Struct. 829 (2007) 208.
[46] T.M. Lankau, Y.C. Wu, J.W. Zou, C.H. Yu, J. Theoret. Comput. Chem. 7 (2008) 13.
[47] L. Yunxiang, Z. Jianwei, W. Hongqing, Y. Qingsen, Z. Huaxin, J. Yongjun, Triangular halogen trimers. A DFT study of the structure, cooperativity, and vibrational properties, J. Phys. Chem. A 11956 (2005) 109.
[48] I. Alkorta, F. Blanco, P.M. Deya, J. Elguero, C. Estarellas, A. Frontera, D. Quinorero, Cooperativity in multiple unusual weak bonds, Theor. Chem. Acc. 1 (2010) 126.
[49] M.J. Frisch, G.W. Trucks, H.B. Schlegel, G.E. Scuseria, M.A. Robb, J.R. Cheeseman, G. Scalmani, V. Barone, B. Mennucci, G.A. Petersson, H. Nakatsuji, M. Caricato, X. Li, H.P. Hratchian, A.F. Izmaylov, J. Bloino, G. Zheng, J.L. Sonnenberg, M. Hada, M. Ehara, K. Toyota, R. Fukuda, J. Hasegawa, M. Ishida, T. Nakajima, Y. Honda, O. Kitao, H. Nakai, T. Vreven, J.A. Montgomery Jr., J.E. Peralta, F. Ogliaro, M. Bearpark, J.J. Heyd, E. Brothers, K.N. Kudin, V. N. Staroverov, R. Kobayashi, J. Normand, K. Raghavachari, A. Rendell, J.C. Burant, S.S. Iyengar, J. Tomasi, M. Cossi, N. Rega, J.M. Millam, M. Klene, J.E. Knox, J.B. Cross, V. Bakken, C. Adamo, J. Jaramillo, R. Gomperts, R.E. Stratmann, O. Yazyev, A.J. Austin, R. Cammi, C. Pomelli, J.W. Ochterski, R.L. Martin, K. Morokuma, V.G. Zakrzewski, G.A. Voth, P. Salvador, J.J. Dannenberg, S. Dapprich, A. D. Daniels, O. Farkas, J.B. Foresman, J.V. Ortiz, J. Cioslowski, D.J. Fox, Gaussian 09, Revision A.02, Gaussian, Inc., Wallingford, CT, 2009.
[50] T.H. Dunning, A road map for the calculation of molecular binding energies, J. Phys. Chem. A 9062 (2000) 104.
[51] T.H. Dunning, Gaussian basis sets for use in correlated molecular calculations. I. The atoms boron through neon and hydrogen, J. Phys. Chem. A 1007 (1989) 90.
[52] K.A. Peterson, D. Figgen, M. Dolg, H. Stoll, Energy-consistent relativistic pseudopotentials and correlation consistent basis sets for the 4d elements Y-Pd, J. Chem. Phys. 124101 (2007) 126.
[53] A.D. Becke, Density-functional exchange-energy approximation with correct asymptotic behavior, Phys. Rev. A 3098 (1988) 38.
[54] A.D. Becke, Density-functional thermochemistry. III. The role of exact exchange, J. Chem. Phys. 9 (8) (1993) 5648.
[55] C. Lee, W. Yang, R.G. Parr, Development of the Colle–Salvetti correlation-energy formula into a functional of the electron density, Phys. Rev. B 37 (1988) 785.
[56] P.J. Stephens, F.J. Devlin, C.F. Chabalowski, M.J. Frish, Ab Initio calculation of vibrational absorption and circular dichroism spectra using density functional force fields, J. Phys. Chem. 11623 (1994) 98.
[57] Y. Zhao, N.E. Schultz, D.G. Truhlar, Design of density functionals by combining the method of constraint satisfaction with parametrization for thermochemistry, thermochemical kinetics, and noncovalent interactions, J. Chem. Theory Comput. 364 (2006) 2.
[58] Y. Zhao, D.G. Truhlar, Density functionals with broad applicability in chemistry, Acc. Chem. Res. 157 (2008) 41.
[59] W. Wang, Y. Zhang, B. Ji, A. Tian, On the correlation between bond-length change and vibrational frequency shift in halogen-bonded complexes, J. Chem. Phys. 224303 (2011) 134.
[60] S.F. Boys, F. Bernardi, Calculation of small molecular interactions by differences of separate total energies – some procedures with reduced errors, Mol. Phys. 553 (1970) 19.
[61] R.F.W. Bader, Atoms in Molecules: A Quantum Theory, Oxford University Press, Oxford, UK, 1990.
[62] F. Biegler-König, J. Schönbohm, D. Bayles, AIM2000 – a program to analyze and visualize atoms in molecules, J. Comput. Chem. 545 (2001) 22.
[63] A.E. Reed, J.E. Carpenter, F. Weinhold, NBO Version 3.1, E.D. Glendening.
[64] A.E. Reed, F.J. Weinhold, Natural localized molecular-orbitals, J. Chem. Phys. 1736 (1985) 83.
[65] A.E. Reed, L.A. Curtiss, F. Weinhold, Intermolecular interactions from a natural bond orbital, donor–acceptor viewpoint, Chem. Rev. 899 (1988) 88.
[66] A.-C.C. Carlsson, J. Gräfenstein, J.L. Laurilla, J. Bergquist, M. Erdélyi, Symmetry of [N—X—N]+ halogen bonds in solution, Chem. Commun. 1458 (2012) 48.
[67] A-C. C. Carlsson, J. Gräfenstein, A. Budnjo, J.L. Laurilla, J. Bergquist, A. Karim, R. Kleinmaier, U. Brath, M. Erdélyi, Symmetric halogen bonding is preferred in solution, J. Am. Chem. Soc. 5706 (2012) 134.
[68] J. Šponer, P. Hobza, Interaction energies of hydrogen-bonded formamide dimer, formamidine dimer, and selected DNA base pairs obtained with large basis sets of atomic orbitals, J. Phys. Chem. A 4592 (2000) 104.
[69] S.J. Grabowski, QTAIM characteristics of halogen bond and related interactions, J. Phys. Chem. A 1838 (2012) 116.
[70] Y. Lu, J. Zou, Y. Wang, Y. Jiang, Q. Yu, Ab initio investigation of the complexes between bromobenzene and several electron donors: some insights into the magnitude and nature of halogen bonding interactions, J. Phys. Chem. A 10781 (2007) 111.
[71] J.-W. Zou, Y.-X. Lu, Q.-S. Yu, H.-X. Zhang, Y.-J. Jiang, Halogen bonding: an AIM analysis of the weak interactions, Chin. J. Chem. 1709 (2006) 24.
[72] Q. Li, H. Yuan, B. Jing, Z. Liu, W. Li, J. Cheng, B. Gong, J. Sun, Theoretical study of halogen bonding between $F_nH_{3-n}CBr$ (n = 0, 1, 2, 3) and HMgH, J. Mol. Struct: THEOCHEM 145 (2010) 942.